

Ultrafast integrated semiconductor optical modulator based on the plasma-dispersion effect

Vilson R. Almeida

Centro Técnico Aeroespacial, São José dos Campos, Sao Paulo 12228, Brazil

Qianfan Xu and Michal Lipson

School of Electrical and Computer Engineering, Cornell University, Ithaca, New York 14853

Received February 22, 2005; revised manuscript received April 4, 2005; accepted May 13, 2005

We demonstrate integrated semiconductor optical devices with ultrafast temporal responses based on the plasma-dispersion effect. The geometry of the devices removes the dependence of the modulation time on the free-carrier dynamics. We present the theoretical analysis of the performance of such devices. We show that a silicon-based device with a free-carrier lifetime of 1.4 ns can be modulated on a time scale of only 20 ps.

The ultrafast operation is verified experimentally. © 2005 Optical Society of America

OCIS codes: 130.2790, 130.3120, 130.4310, 130.5990, 190.7110, 190.4390.

Electro-optical and all-optical semiconductor devices permit external control of on-chip optoelectronic circuits. Recently, several devices based on the plasma-dispersion effect have been proposed and demonstrated with high performance.^{1–5} However, the temporal response of these semiconductor devices is dependent upon the dynamics of the free-carrier diffusion and recombination processes in the semiconductor material used as the waveguide core, severely limiting the speed of devices. Here we present a novel class of optical devices based on the plasma-dispersion effect with ultrafast temporal response and minimal dependence on the free-carrier dynamics.

Figure 1(a) shows the schematic of the proposed device architecture. It is a Mach–Zehnder interferometer (MZI) comprising sections of wide and narrow waveguides. The device is designed to be submitted to either an electrical or an optical excitation (pump) that generates free carriers, which in turn modulates the probe by means of the plasma-dispersion effect.^{4,6} For simplicity, here we analyze only the all-optical approach, in which the pump excitation is composed of an ultrafast optical pump beam launched in plane, counterpropagating with respect to the optical probe beam, which is cw at its input. Figure 1(a) illustrates the counterpropagating scheme for pump and probe beams. As the pump beam pulse propagates from the input waveguide into the device, it is split into two pulses with the same optical power (50/50 split).

The principle of operation of the device relies on the fact that the pulsed pump beam induces refractive index change only in the narrow arm section because of the strong confinement of the pump beam therein, which causes an optical intensity strong enough to induce two-photon absorption (TPA). TPA is responsible for photogeneration of free carriers, which in turn alter the refractive index of the material through the free-carrier plasma effect. In contrast, in the wide arm section the optical intensity is relatively low, and TPA is negligible. The fast response of the device is based on the fact that the probe beam modulation time is determined by the difference in time of the index modulation in each

arm. The phase shift of the cw probe beam of $\Delta n_g L$ in arm 1 occurs when the pump pulse propagates in the narrower waveguide, earlier than it occurs in arm 2. A phase difference occurs only when arm 1 experiences a phase shift before arm 2. Otherwise both arms introduce the same total optical phase due to their symmetry. Therefore both turn-on and turn-off times are determined by the time it takes for each of the counterpropagating (pump and probe) beams to propagate through a half-length of the interferometer arm, which gives $\Delta\tau_{\text{arm}} = n_g L/c$. For example, a silicon interferometer with $n_g = 4$ and an arm length of $L = 2$ mm induces a probe beam intensity modulation within a time of only $\Delta\tau_{\text{arm}} = 26$ ps. This is in contrast to the typical modulation time of similar devices determined by free-carrier recombination dynamics, of the order of hundreds of picoseconds.^{4,6} If the interferometer is balanced ($\phi_{\text{MZ}} = 0$), the induced phase change will cause a decrease in probe beam intensity, whereas if the interferometer is unbalanced with $\phi_{\text{MZ}} = \pi$ rad, the induced phase change will cause an increase in intensity.

A phase imbalance between the two arms usually introduces a temperature and wavelength dependence. However, in this case, since the effective index

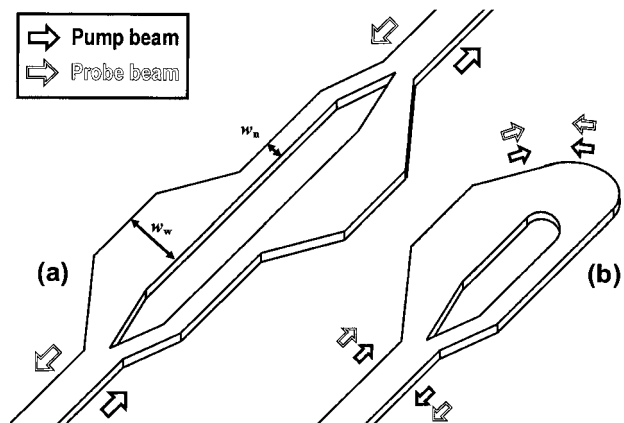


Fig. 1. Schematics of ultrafast semiconductor optical devices, showing the (a) Mach–Zehnder and (b) Sagnac interferometer approaches. Pump and probe beams are counterpropagating.

difference between wide and narrow waveguides is large ($\Delta n_{\text{eff}} \cong 0.48$), an unperturbed phase unbalance of $\phi_{\text{MZ}} = \pi$ rad is obtained by an arm asymmetry of only $\Delta L = \lambda_0 / (2\Delta n_{\text{eff}}) \cong 1.6 \mu\text{m}$; considering a thermo-optic coefficient of $\partial n_{\text{Si}} / \partial T = 1.86 \times 10^{-4} \text{ K}^{-1}$,⁷ this asymmetry causes a negligible temperature dependence for the optical phase imbalance of $\partial \phi_{\text{MZ}} / \partial T = -9.7 \times 10^{-5} \text{ rad/K}$. Additionally, for this arm length asymmetry, a weak wavelength dependence of $\partial \phi_{\text{MZ}} / \partial \lambda = -2 \times 10^{-3} \text{ rad/nm}$ is also expected.

Below we numerically analyze the all-optical ultrafast modulator, assuming silicon for the waveguide core ($n_{\text{Si}} = 3.48$) and SiO_2 ($n_{\text{SiO}_2} = 1.46$) for the surrounding cladding. Simulations were carried out by using a finite-difference method implementation including nonlinear optical effects such as TPA and the plasma-dispersion effect. The waveguide dimensions are height, $h_w = 250 \text{ nm}$; wide-waveguide width, $w_w = 2,500 \text{ nm}$; and narrow-waveguide width, $w_n = 450 \text{ nm}$; the wavelength for the probe and pump are assumed to be distinct and are around $\lambda_0 = 1550 \text{ nm}$ in vacuum. Assuming nonlinear optical coefficients for silicon of $\beta_{\text{TPA}} = 8 \times 10^{-12} \text{ m/W}$ and $n_2 = 4.5 \times 10^{-18} \text{ m}^2/\text{W}$,⁸ we simulate the temporal response for the probe beam by using pump pulses with $E_{\text{pump}} = 50 \text{ pJ}$ of energy and temporal width of $\tau_{\text{pump}} = 5 \text{ ps}$; we consider $L = 2 \text{ mm}$ and a free-carrier lifetime of $\tau_{\text{fc}} = 1.4 \text{ ns}$.⁹ The probe modulation is shown in Figs. 2(a) and 2(b) for the unperturbed balanced ($\phi_{\text{MZ}} = 0$) and unbalanced ($\phi_{\text{MZ}} = \pi$ rad) arms, respectively. We simulated the response of the device for two difference pump beam pulse interval, $\tau_{\text{int}} = 0.5 \text{ ns}$ and the (dotted curves) $\tau_{\text{int}} = 1.5 \text{ ns}$. Figure 2 shows a fast modulation time of 20 ps, orders of magnitude shorter than the free-carrier lifetime. One can see that the modulation time stays constant regardless of the unperturbed phase unbalance and of the pump beam pulse interval. The effect of the free-carrier absorption on the probe beam modulation as a function of the pump beam pulse interval can also be observed; the shorter the τ_{int} , the higher the average free-carrier concentration and absorption. This free-carrier absorption effect can be decreased by using a configuration that reduces free-carrier accumulation, such as the recently demonstrated p-i-n configuration in a reverse biased p-i-n structure.¹⁰ The device is robust, with respect to the modulation depth, to small changes in pump power. A 10% variation in pump

power is expected to cause very small variations in the modulation depth for device operation around both the balanced (1.2%) and the unbalanced (2.2%) Mach-Zehnder arms.

To verify experimentally the ultrafast response of the all-optical device, we fabricated the MZI shown in Fig. 1(a) on a silicon-on-insulator platform by using the same processes described in Ref. 11. The fabricated device has geometric parameters similar to those described in the simulations. Figure 3(a) shows the microscopic image of the splitting and narrow-wide waveguide transition regions of the fabricated MZI; 1.5-ps pump pulses at $\lambda_{\text{pump}} = 1474 \text{ nm}$ are generated by an optical parametric oscillator and coupled to the waveguide through the nanotaper.¹¹ The input pump pulse energy is about 200 pJ. The counterpropagating probe beam is generated by a cw tunable laser set at $\lambda_{\text{probe}} = 1540 \text{ nm}$. The transmission waveforms of the probe are obtained from a photodetector with a nominal rise and fall time of 30 ps. The waveforms are shown in Figs. 3(b) and 3(c) for modulators with balanced and unbalanced arms, respectively. The total arm length L is 4 mm for the modulator with balanced arms and 3 mm for the modulator with unbalanced arms. We used devices slightly longer than the one that was simulated, such that the measured dynamics are not severely limited by the detector response time (of the order of 30 ps). We measured a modulation time of about an order of magnitude shorter than the typical free-carrier lifetime in these waveguides.⁹ The shapes of the waveforms agree well with the simulations. As expected, the modulator with unbalanced arms has faster modulation than the device with balanced arms, owing to the shorter arm length. The input pump pulse energy is higher than that used in simulations because of insertion losses from the coupling between optical fiber and waveguide as well as the transmission losses in the waveguides and in the splitter. In Fig. 3(b) one can see that the modulation depth is limited to about 5 dB, mainly because the splitting ratio of the splitter is not ideally 50:50. The observed modulation depth is also partially limited by the time-averaging effect of the detector because of its limited time response.

The same device's principle of operation can be achieved by using a Sagnac interferometer approach, as seen in Fig. 1(b). In the Sagnac approach, the pump and probe beams automatically present both

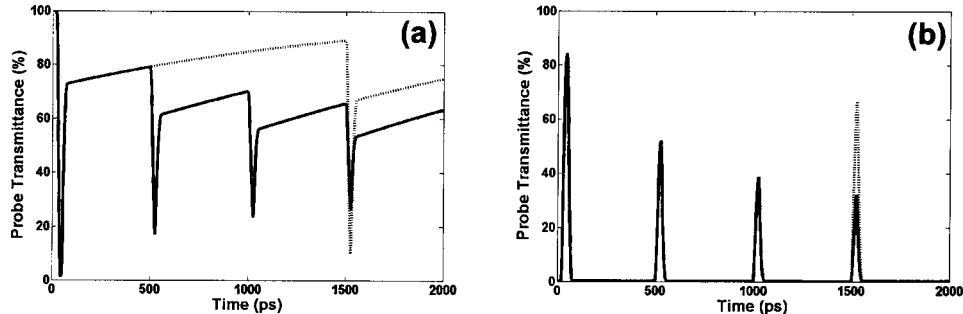


Fig. 2. Simulated temporal response of an ultrafast Mach-Zehnder all-optical device for (a) balanced ($\phi_{\text{MZ}} = 0$) and (b) unbalanced ($\phi_{\text{MZ}} = \pi$ rad) arms. Solid and dotted curves represent pump pulse intervals τ_{int} of 0.5 and 1.5 ns, respectively.

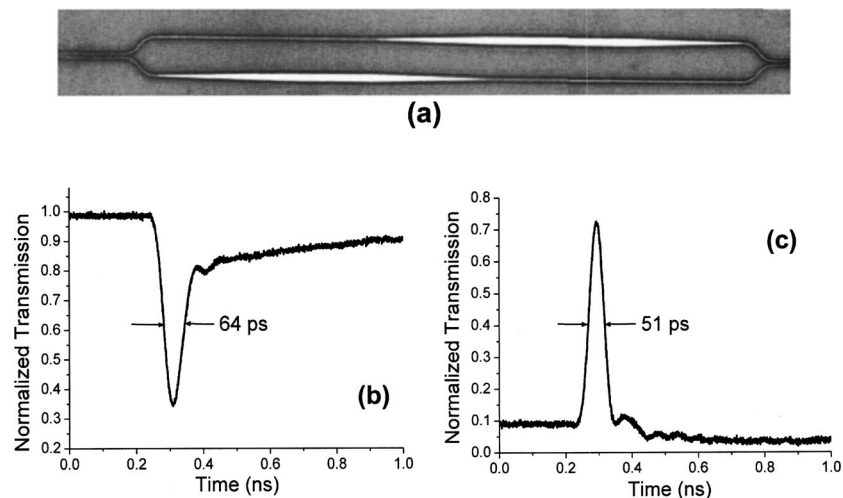


Fig. 3. (a) Microscopic image of the splitting region and the narrow-wide waveguide transition region of the MZI. (b), (c) Measured temporal response of the MZI ultrafast modulators with (b) balanced arms ($L=4$ mm) and (c) slightly unbalanced (π rad) arms ($L=3$ mm).

counterpropagating and copropagating components inside the interferometer loop, as seen in Fig. 1(b).

In conclusion, we show both theoretically and experimentally a novel architecture for achieving ultrafast optical modulation on semiconductor devices based on the plasma-dispersion effect.

V. R. Almeida acknowledges support from the Brazilian Defense Ministry. This work has been partially carried out as part of the Interconnect Focus Center Research Program at Cornell University, support in part by the Microelectronics Advanced Research Corporation (MARCO), its participating companies, and DARPA under contract 2003-IT-674. The authors acknowledge support by the National Science Foundation (NSF) under contract ECS-0300387. We thank Gernot Pomrenke, AFOSR, for supporting the work through grant STTR (FA9550-04-C-0097). The devices were fabricated at the Cornell Nano-Scale Science & Technology Facility (a member of the National Nanofabrication Users Network), which is supported by the National Science Foundation under grant ECS-9731293, its users, and Cornell University and Industrial Affiliates. V. R. Almeida's e-mail address is vra2@cornell.edu. M. Lipson's e-mail is mlipson@cornell.edu.

References

1. R. A. Soref and B. R. Bennett, Proc. SPIE **704**, 32 (1986).
2. T. A. Ibrahim, W. Cao, Y. Kim, J. Li, J. Goldhar, P.-T. Ho, and Chi H. Lee, IEEE Photon. Technol. Lett. **15**, 36 (2003).
3. V. Van, T. A. Ibrahim, K. Ritter, P. P. Absil, F. G. Johnson, R. Grover, J. Goldhar, and P.-T. Ho, IEEE Photon. Technol. Lett. **14**, 74 (2002).
4. V. R. Almeida, C. A. Barrios, and R. R. Panepucci, Nature **431**, 1081 (2004).
5. V. R. Almeida, C. A. Barrios, R. R. Panepucci, M. A. Foster, D. G. Ouzounov, A. L. Gaeta, and M. Lipson, Opt. Lett. **29**, 2867 (2004).
6. A. Liu, R. Jones, L. Liao, D. Samara-Rubio, D. Rubin, O. Cohen, R. Nicolaescu, and M. Paniccia, Nature **427**, 615 (2004).
7. G. Cocorullo and I. Rendina, Electron. Lett. **28**, 83 (1992).
8. M. Dinu, F. Quochi, and H. Garcia, Appl. Phys. Lett. **82**, 2954 (2003).
9. Q. Xu, V. R. Almeida, and M. Lipson, Opt. Lett. **30**, 35 (2005).
10. H. Rong, A. Liu, R. Jones, O. Cohen, D. Hak, R. Nicolaescu, A. Fang, and M. Paniccia, Nature **433**, 292 (2005).
11. V. Almeida, R. R. Panepucci, and M. Lipson, Opt. Lett. **28**, 1302 (2003).